Supporting Information

Betts et al. 10.1073/pnas.1712452115

SI Materials and Methods

mAbs and Flow Cytometry. Fluorochrome-conjugated anti-mouse or -human monoclonal antibodies included anti-CD3, CD4, CD8, CD25, CD127, Foxp3, B220, $H2K^b$, CD45.1, T-bet, IFNγ, IL-4, IL-5, IL-10, IL-17, $\alpha_4\beta_7$, CXCR3, CCR6, streptavidin, phosphorylated STAT1, phosphorylated STAT3 Y705, and phosphorylated STAT5 Y694 (BD Biosciences; eBioscience; Cell Signaling Technology). As indicated, CFSE was used in standard proliferation assays. Live/Dead Fixable Yellow Dead Cell Stain (Life Technologies) was used to determine viability. Live events were acquired on a FACSCanto or LSRII flow cytometer (FlowJo software, version 7.6.4; TreeStar).

Human T Cell and NK-Cell in Vitro Experiments.

Allogeneic Mixed Leukocyte Reaction. Human, DC-allostimulated T cell proliferation was tested in standard, 5-d mixed leukocyte reactions (MLRs) (DC:T cell ratio 1:30). DMSO or pacritinib (2.5 μM) was added once on day 0. T cell proliferation was determined by a colorimetric assay according to the manufacturer's instructions (CellTiter96 Aqueous One Solution Cell Proliferation Assay MTS; Promega) (18). As indicated, intracellular T-bet, IFNγ, and/or IL-4 was quantified by flow cytometry on day +5 following a 4- to 5-h stimulation with phorbol 12-myristate 13-acetate/ionomycin.

NK-cell proliferation. Magnetic bead purified NK cells were cultured with allogeneic, immature dendritic cells or a cytokine mixture of IL-2 (200 IU/mL) and IL-15 (10 ng/mL). Medium was supplemented with additional cytokines on days +2 and +4. Pacritinib (2.5 μM), ruxolitinib (1 μM), or DMSO vehicle control was added once on day 0. NK-cell proliferation was measured by a colorimetric assay on day +5.

NK-cell tumor lysis. Human NK cells were cultured with HLA class I-deficient K562 targets at the described ratios. Pacritinib (2.5 μM), ruxolitinib (1 μM), or DMSO vehicle control was added to the cultures. NK-cell lytic function was measured after 4 h.

Protein Phosphorylation Experiments. For STAT1, STAT3, and STAT5 phosphorylation, human T cells were serum-starved in RPMI treated with DMSO, pacritinib (2.5 μM), or ruxolitinib (1 μM) as indicated (17) for 4 h. IL-6–induced pSTAT3, IL-2–induced pSTAT5 (Y694), or IFNγ-induced pSTAT1 was measured by flow cytometry as described (18).

iTreg Experiments. Human iTregs were generated as previously described (18) in the presence of DMSO or pacritinib (2.5 μM). On day +5, iTregs were isolated and washed to minimize drug carryover as reported (18). The T cells were harvested and surface-stained for CD3, CD4, CD25, and CD127, followed by fixation and permeabilization (eBioscience) and then Foxp3 staining. The iTregs were identified as CD4+, CD127−, CD25+, and Foxp3+ (18). Activated CD4+ and Tconv cells were phenotypically characterized by expression of CD25 and CD127 (18). To test suppressive potency, the purified iTregs were titrated against allo-MLRs consisting of 5×10^4 responder CD4+ CD25− T cells from the iTreg donor and 1.6×10^3 DCs from the original stimulator donor. T cell proliferation was determined by pulsing cells with 1 uCi/well 3H-thymidine during the last 18 h of culture (18). The iTreg suppression cultures were not treated with DMSO or pacritinib.

RORγT RT-PCR. Th17 differentiation was assessed among CD4+ T cells by RT-PCR. Naive CD4+ T cells were purified by magnetic bead separation (Miltenyi Biotec) and stimulated with allogeneic DCs (DC:T cell ratio 1:30). The cocultures were treated with pacritinib (2.5 μM) or DMSO. The media were supplemented with IL-6, TGFβ, and anti-IFNγ as described (5). After 5 d, the cells were harvested and total RNA was extracted. Assay primer selection and RT-PCR procedure were carried out as described (5).

B- and T Cell Coculture Cytokines. Healthy donor B and T cells were stimulated with goat anti-human IgM and superantigens in the presence of pacritinib or vehicle control (BioSeek). Cytokines were measured after 72 h of incubation and analyzed as described (26).

In Vivo Human CTL Generation. To generate CD8+ CTL in vivo, mice were transplanted with 30×10^6 human PBMCs and also received an inoculum of irradiated U937 cells (10×10^6) on day 0 and +7 as described (18). A control cohort of mice received PBMCs alone and were not vaccinated with tumor. Mice did not receive skin grafts for these experiments. Mice were treated with pacritinib (100 mg/kg), ruxolitinib (30 mg/kg) (4), or vehicle twice a day starting on day 0. On days +10–12, the mice were humanely euthanized, and the spleens were harvested. Human CD8+ T cells were isolated from single-cell spleen suspension using magnetic bead isolation. Tumor lysis assays were performed in vitro (18).

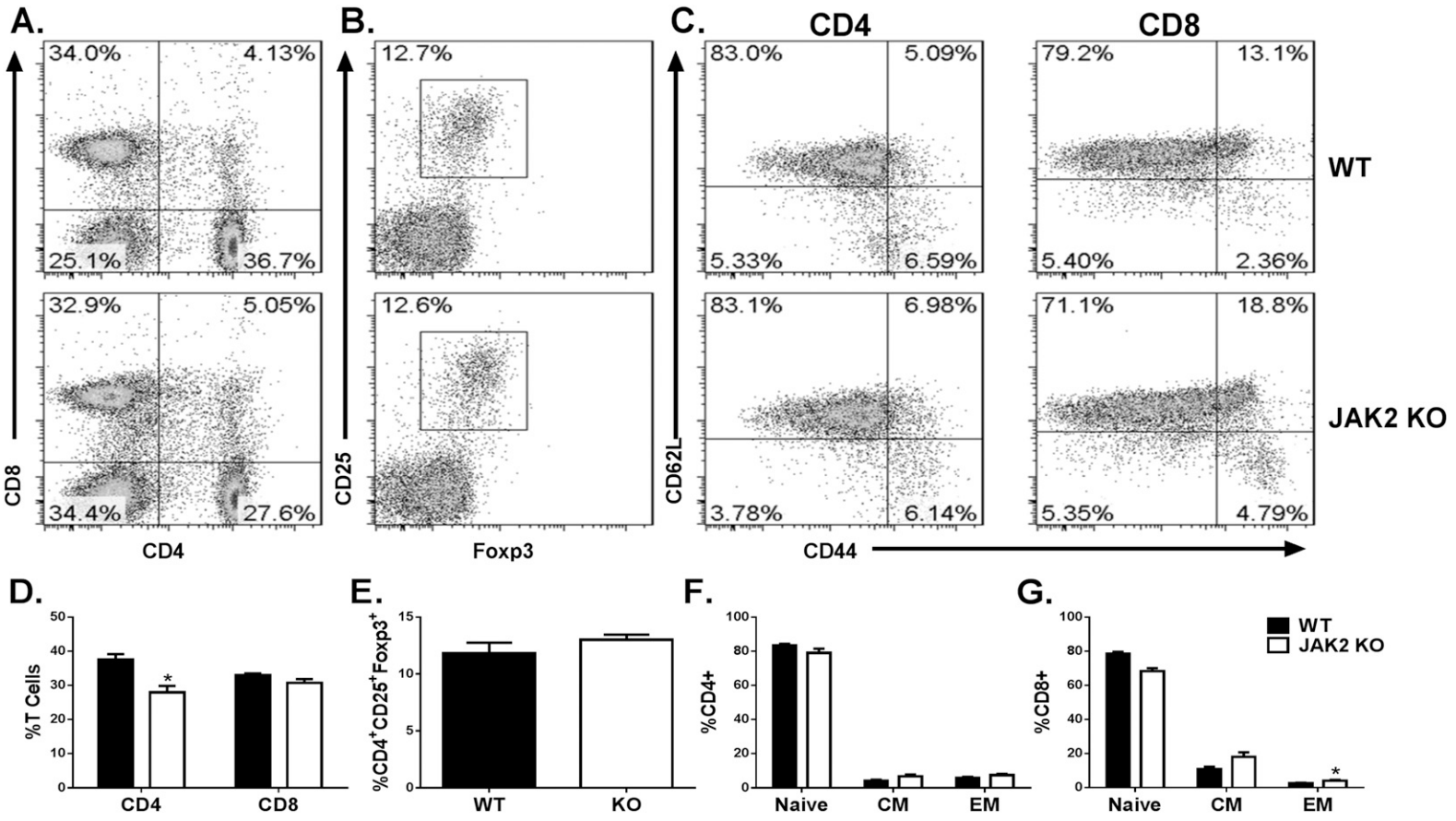

Fig. S1. Comparable immunological phenotype of WT and JAK2 KO mice. Spleens from naive WT B6 or JAK2 KO mice were harvested and stained for flow cytometry. Representative percentages of CD4+ and CD8+ T cells (*A*), CD4+CD25+Foxp3+ nTregs (*B*), and CD4+ (*Left*) or CD8+ (*Right*) memory markers (*C*) are shown. Corresponding summary graphs are shown below each image (*D*–*G*). *$P < 0.05$.

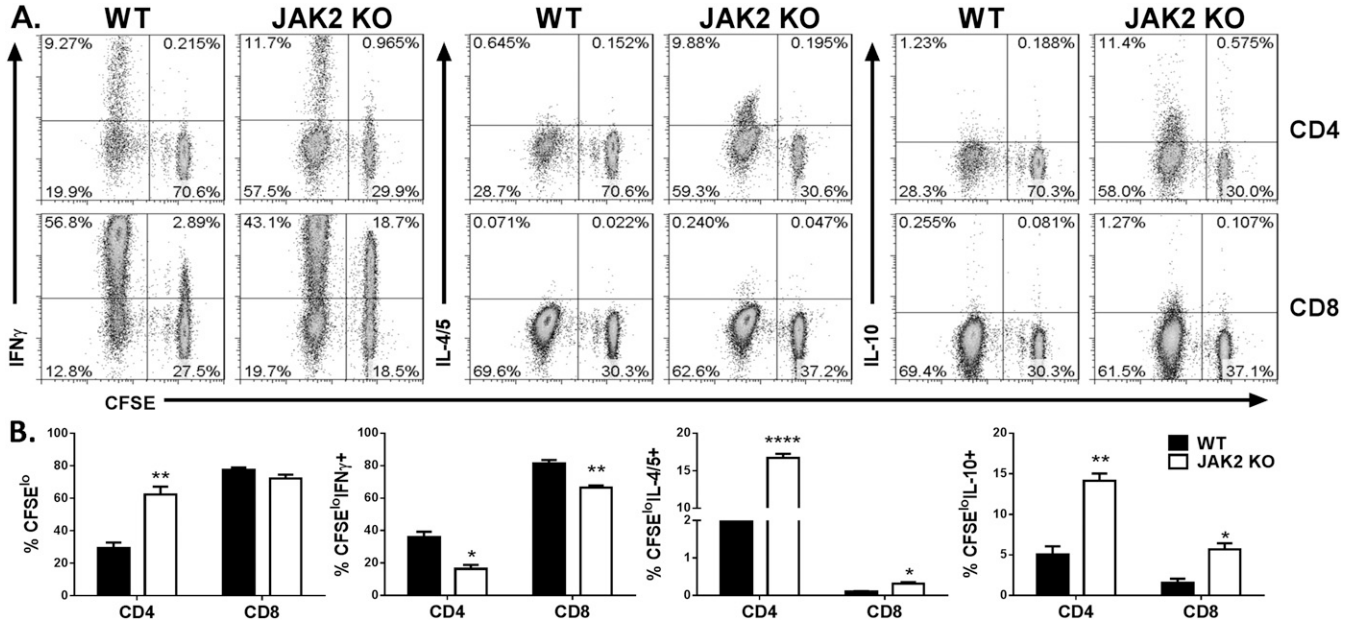

Fig. S2. JAK2 inhibits Th2 and Treg polarization in vitro. Purified CD4+ and CD8+ T cells (2×10^5/well) from either WT B6 or JAK2 KO mice were labeled with CFSE, plated in triplicate wells, and cultured with T cell-depleted BALB/c splenocytes (6×10^5/well) for 5 d. Cells were then harvested, stained for surface and intracellular markers, and analyzed by flow cytometry. (*A*) Representative flow cytometry figures for percentages of IFNγ (*Left*), IL-4/5 (*Middle*), and IL-10 (*Right*) are shown. (*B*) Graphical displays for percentages of CD4+, CD8+ IFNγ, IL-4/5, and IL-10 (*Left* to *Right*) among CFSE-diluted T cells are shown. Flow cytometry data are depicted for one representative mouse per group (*A*) or mean + SD of percentages with three mice per group (*B*). Two replicate experiments were performed for a total of six mice per group. *$P < 0.05$; **$P < 0.01$; ****$P < 0.0001$.

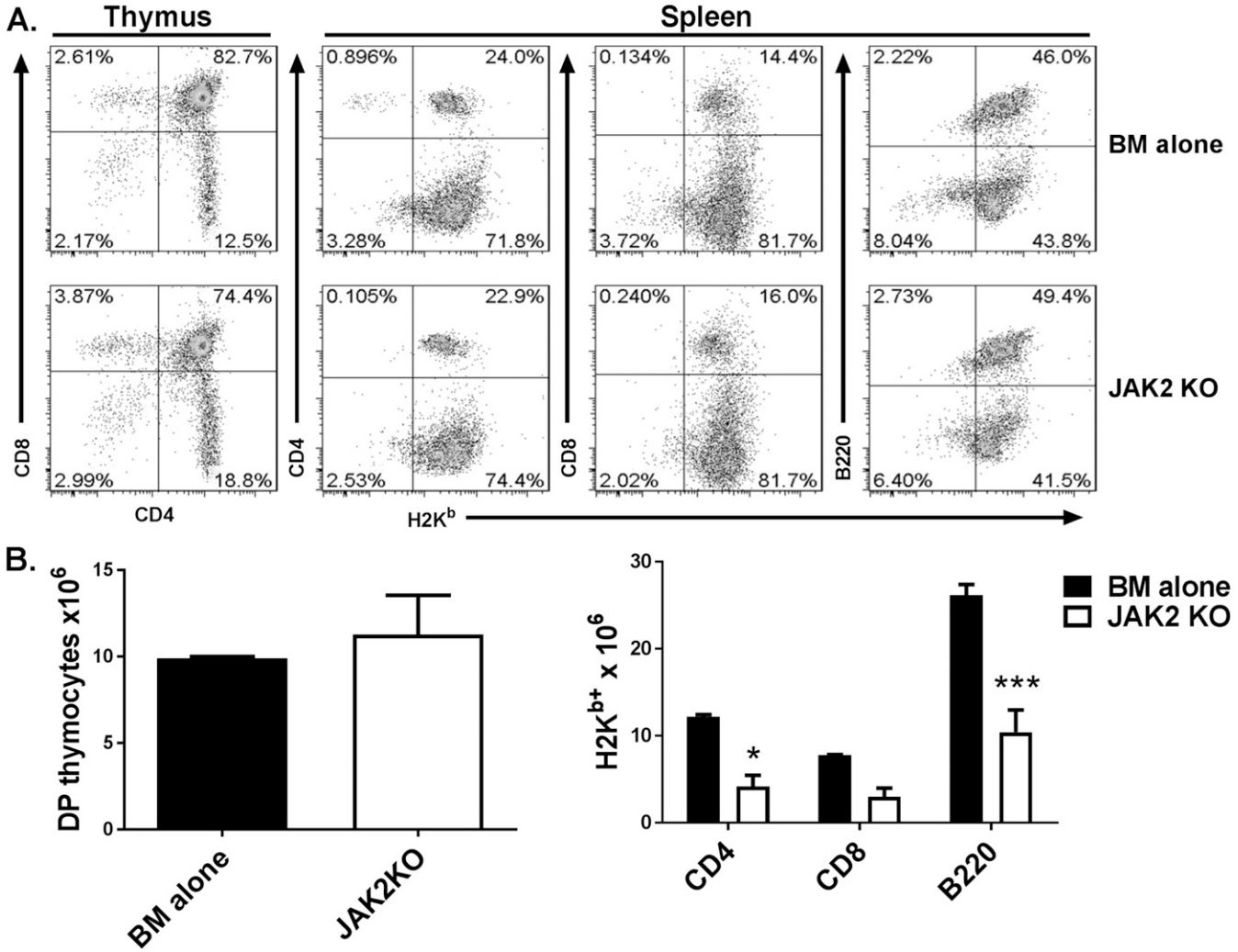

Fig. S3. Immune reconstitution in recipient thymus and spleen. Lethally irradiated BALB/c mice were transplanted with 5×10^6 TCD-BM alone or plus 1×10^6 purified T cells from WT B6 or JAK2 KO mice. After 80 d, the remaining recipient mice were killed, and the spleen and thymus were harvested. (*A*) Flow cytometry data are depicted for one representative mouse per group and percentages of CD4+CD8+ double-positive T cells in the thymus (*Left*) and donor CD4+, CD8+, and B220+ cells in the spleen (*Right*) are shown. (*B*) Absolute numbers for double-positive thymocytes (*Left*) and donor CD4+, CD8+, and B220+ in the spleen (*Right*) are shown. Data shown were taken from one of three replicate experiments with a total of six BALB/c mice that received TCD-BM alone and 15 BALB/c mice per group that received T cells. $*P < 0.05$; $***P < 0.001$.

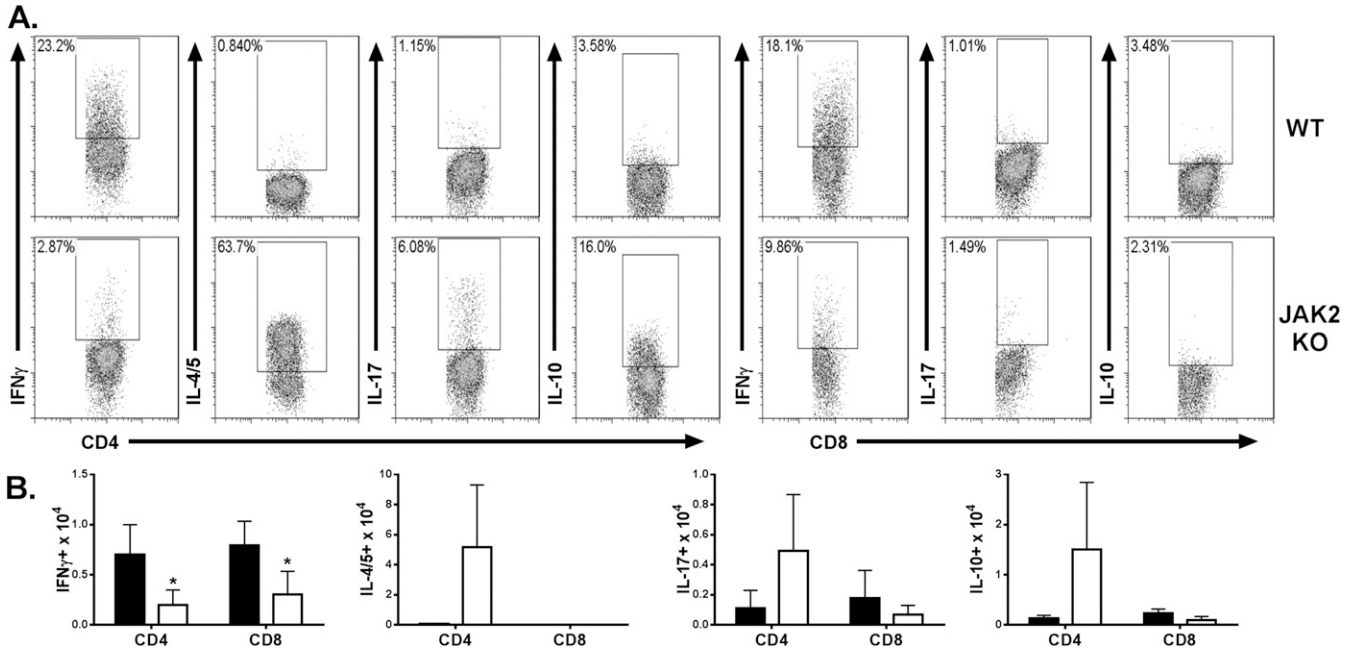

Fig. S4. Donor T cells deficient for JAK2 are prone to Th2 and Treg polarization in the liver. Lethally irradiated BALB/c mice were transplanted with 5×10^6 Ly5.1+ TCD-BM alone or plus 1×10^6 purified T cells (Ly5.2+) from WT B6 or JAK2 KO mice. Fourteen days post-BMT, recipient livers were collected, and mononuclear cells were isolated and stained for surface and intracellular markers for analysis by flow cytometry. (*A*) Flow cytometry data are depicted for one representative mouse per group for IFNγ+, IL-4/5+, IL-17+, or IL-10+ among gated $H2K^b$+Ly5.1-CD4+ or CD8+ cells in the liver. (*B*) Absolute numbers +SD of CD4+ or CD8+ T cells positive for IFNγ, IL-4/5, IL-17, or IL-10 among gated H2Kb+Ly5.1-CD4+ or CD8+ cells in the liver are shown. Representative data for one of three replicate experiments with four mice per group are shown. The total number of mice analyzed in these experiments in the WT group was nine, and the total number in the JAK2 KO group was 11. $*P < 0.05$.

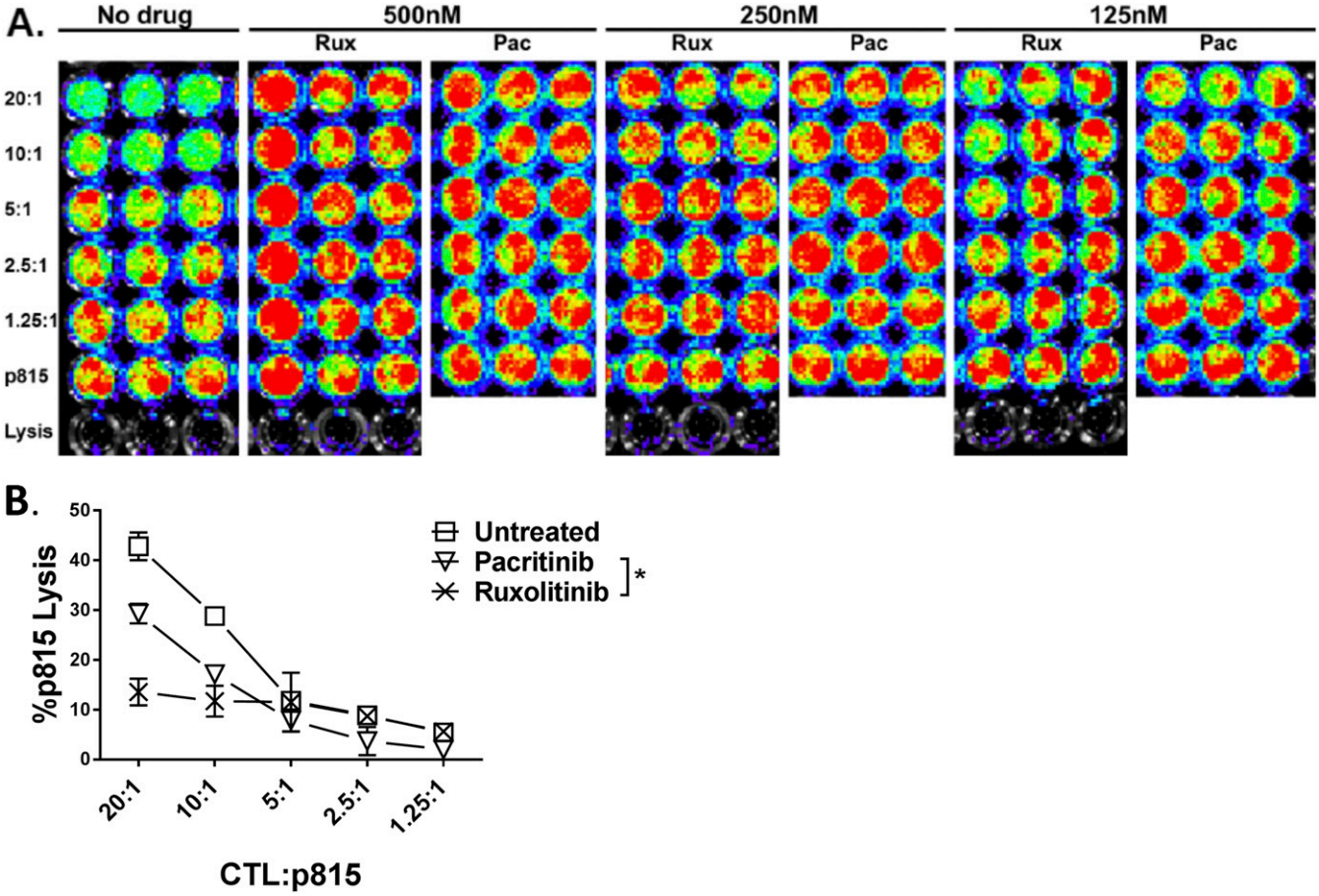

Fig. S5. Effect of JAK2 or JAK1/2 inhibition on murine CTL function. Purified CD8+ T cells from WT B6 mice, and purified CD11c+ DCs from BALB/c mice were plated at a 10:1 ratio (1.5×10^5 CD8:0.15×10^5 DCs/well) and were treated with pacritinib (JAK2 inhibitor) or ruxolitinib (JAK1/2 inhibitor) with 1 μM, 500 nM, 250 nM, 125 nM, or no inhibitor. After 5 d, the respective groups of cells were harvested and replated with p815 luciferase-transduced cells in triplicate wells at ratios of 20:1, 10:1, 5:1, 2.5:1, 1.25:1, 0:1, or 0:1 + cell lysis (T cell:5,000 p815 cells/well) and incubated for 5 h. Cells were then incubated with luciferin and imaged, and the BLI per well was recorded. Representative images for each group (*A*) and a graphical representation of the average BLI + SD of untreated, 125 nM ruxolitinib, or 125 nM pacritinib (*B*) are shown. $^*P < 0.05$. Pac, pacritinib.

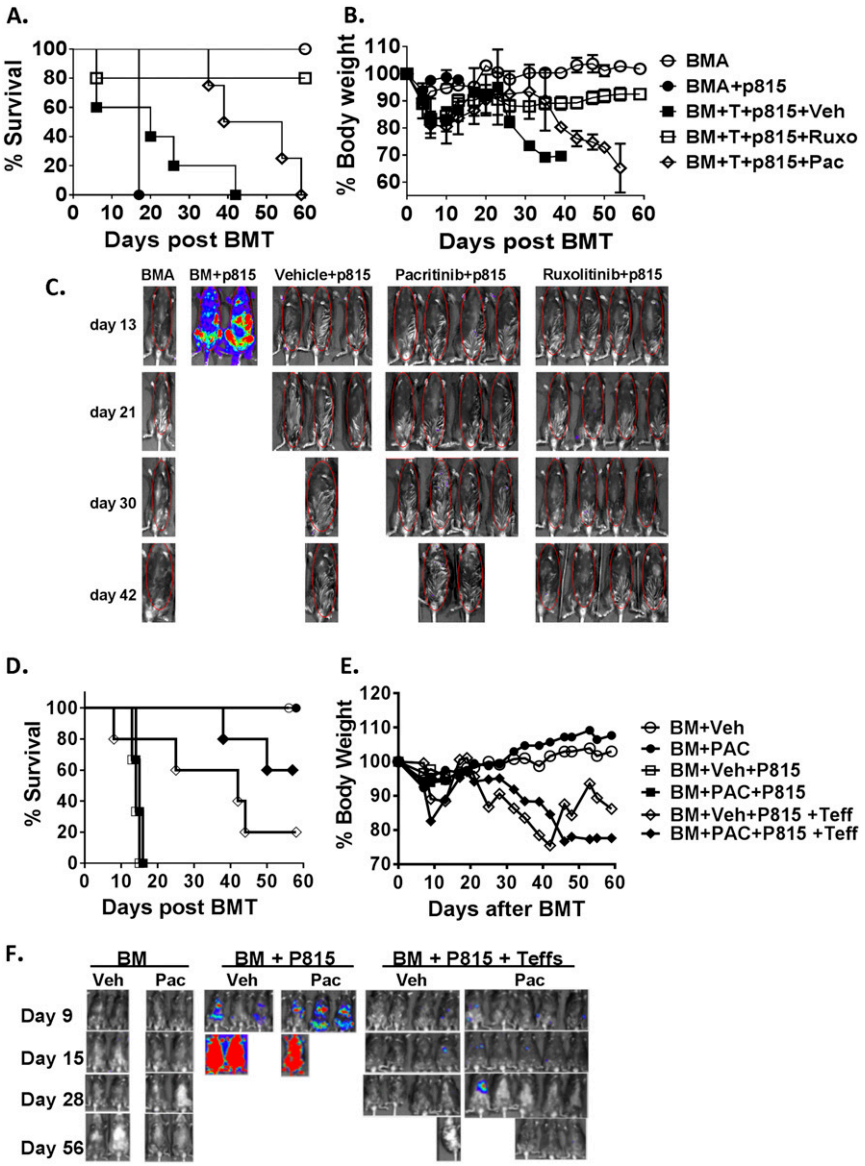

Fig. S6. Effect of JAK2 or JAK1/2 inhibition on murine GVL. Lethally irradiated (B6 × DBA2)F1 mice received TCB-BM alone or with 3×10^6 B6 T cells and 5×10^3 luciferase-transduced P815. Ruxolitinib (JAK1/2 inhibitor, 30 mg/kg twice a day), pacritinib, or vehicle was administered as described. Recipient survival (*A*), weight loss (*B*), and tumor progress (*C*) from one representative experiment with five mice per group are shown. Lethally irradiated (B6 × DBA2)F1 mice received TCB-BM alone or with 3×10^6 B6 T cells and 5×10^3 luciferase-transduced P815. Pacritinib or vehicle was administered as described. Pacritinib treatment plus BM without T cell controls were included. Recipient survival (*D*), weight loss (*E*), and tumor progress (*F*) are shown. Data represent one of two experiments with similar setting. Pac, pacritinib; Veh, vehicle.

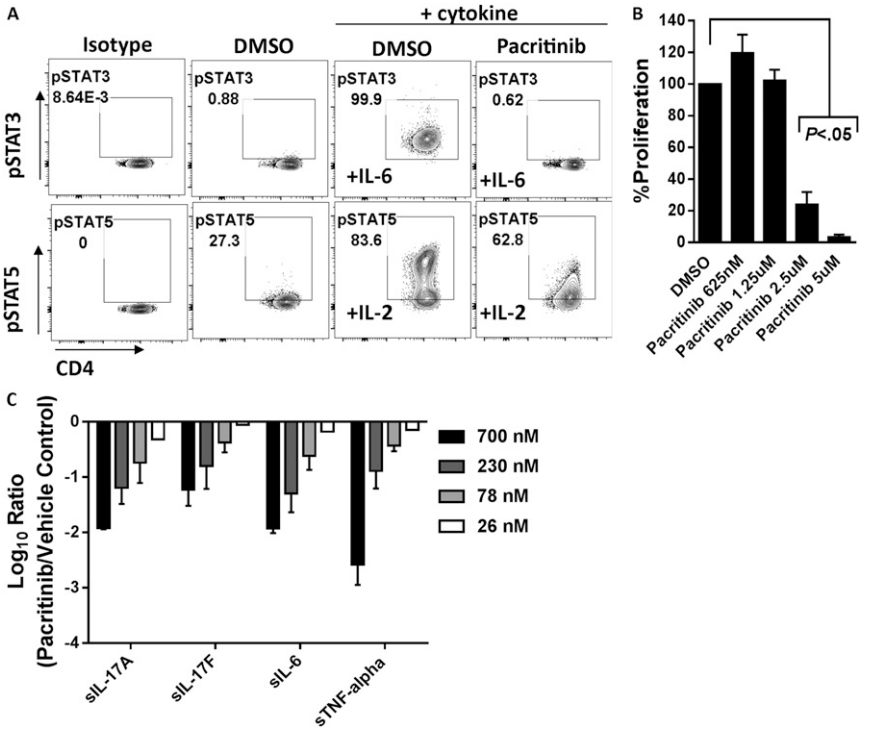

Fig. S7. Impact of JAK2 inhibition by pacritinib on human T cell proliferation, protein phosphorylation, and cytokine production. (*A*) Pacritinib (2.5 μM) reduces STAT3 activity by IL-6 (4,000 IU/mL × 15 min) in CD4+ T cells, yet permits IL-2–induced (50 IU/mL × 15 min) STAT5 phosphorylation (representative contour plots, one of two experiments). (*B*) Pacritinib impairs T cell proliferation in 5-d allo-MLRs (DC:T cell ratio 1:30, $n = 3$ experiments in triplicate). Graph shows mean T cell proliferation ±SEM, measured by colorimetric assay. (*C*) Bar graph shows dose-dependent suppression of soluble IL-17A, IL-17F, IL-6, and TNF-alpha by various concentrations of pacritinib in culture with purified human B and T cells from at least three donors, stimulated by anti-human IgM and superantigens. Cytokines were measured after 72 h of incubation and analyzed as described (26).

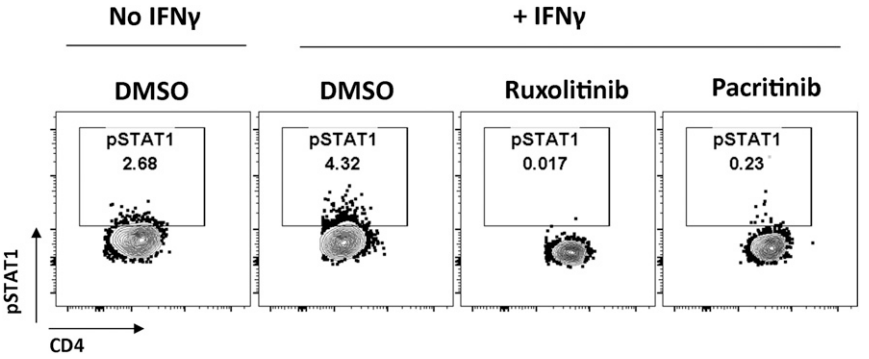

Fig. S8. JAK2 inhibitors reduce STAT1 phosphorylation in IFNγ-stimulated human T cells. Peripheral blood mononuclear cells were briefly activated with CD3/CD28 beads at a ratio of 2:1 for 24 h. The beads were discarded, and the cells were cultured in serum-free RPMI treated with DMSO, ruxolitinib (1 μM), or pacritinib (2.5 μM). After 2 h, the cells were stimulated with IFNγ (200 ng/mL) for 25 min. The cells were then fixed, permeabilized, and stained for CD3, CD4, and pSTAT1. pSTAT1 expression among the stimulated CD4+ T cells was quantified by flow cytometry. Representative contour plots are shown for each experimental condition. $n = 2$ independent experiments with similar results.

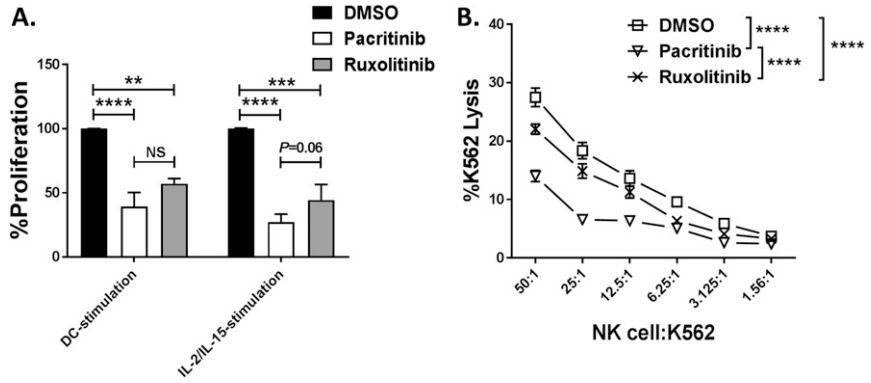

Fig. S9. Effect of JAK inhibition on human NK-cell proliferation and function. Magnetic bead purified NK cells were cultured with allogeneic, immature DCs or a cytokine mixture of IL-2 (200 IU/mL) and IL-15 (10 ng/mL). Medium was supplemented with additional cytokines on days +2 and +4. Pacritinib (2.5 μM), ruxolitinib (1 μM), or DMSO vehicle control was added once on day 0. (*A*) NK-cell proliferation was measured by a colorimetric assay on day +5. (*B*) Human NK cells were cultured with K562 targets at the described ratios. Pacritinib (2.5 μM), ruxolitinib (1 μM), or DMSO vehicle control was added to the cultures. NK-cell lytic function was measured after 4 h. $^{**}P < 0.01$, $^{***}P < 0.001$, $^{****}P < 0.0001$. NS, not significant.